



## DIPLOMA WORK 2007

<b>Title:</b> Optimal operation and control of Kaibel distillation column	<b>Subject (3-4 words):</b> Distillation Kaibel
<b>Author:</b> Petter Hande Haugen	<b>Carried out through:</b> 19.01.2007 – 15.06.2007
<b>Advisor:</b> Sigurd Skogestad <b>Co-advisor:</b> Jens Strandberg	<b><u>Number of pages</u></b>  <b>Hovedrapport:</b> 32 <b>Bilag:</b> 3
<b>External advisor:</b> -	
<b>ABSTRACT</b>  <b>Goal of work (key words):</b>  The aim of this thesis was to investigate the effect of certain parameters on the optimal operation and the corresponding temperature profile of the distillation column. The temperature profile is important when considering a self-optimising control scheme. The simulations will be done in the process simulator Aspen Plus.  A laboratory scale column had been built at NTNU, and samples taken from the column were to be analysed, and compared to the results of the simulations. This, in an attempt to support the simulation results.  <b>Conclusions and recommendations (key words):</b>  The simulations were carried out as planned, and some well-known distillation facts were established. Especially interesting was the effect of the vapour split on the column's performance.  Unfortunately, the analysis of the laboratory column could not be performed. The apparatus available did not perform within accuracy, and it was decided to not carry out further testing.	
<b>I declare that this is an independent work according to the exam regulations of the Norwegian University of Science and Technology</b>	
<b>Date and signature:</b> .....	

## **Abstract**

The Kaibel distillation column is a fully thermally coupled column, capable of separating four products in a single column shell with a single reboiler. This thesis aims to investigate the effect of certain parameters on the optimal operation and the corresponding temperature profile of the column. The temperature profile associated with optimality is important when considering self-optimising control. An attempt at validating the results of the simulations by analysis of samples from a real column experiment was made.

Simulations of the column were performed in Aspen Plus. The results of the simulations established some well-known facts about distillation and helped validate the simulation model. The effect of reflux rate, number of column stages and the effect of the vapour split were investigated. The first two showed only moderate changes in temperature profile, while the vapour split showed a more substantial effect.

The validation of the simulation results by performing a real laboratory column experiment did not happen as planned. This was due to problems with the analysis apparatus, a gas chromatograph. Analysis of the experimental results was not carried out as planned, and neither a useful result nor a conclusion can be drawn from this.

## **Preface**

This thesis has been written as part of my Master's Degree at the Department of Chemical Engineering, Norwegian University of Science and Technology (NTNU). The work has been carried out during the spring and early summer of 2007. Long, sometimes tedious hours, in the laboratory has been a challenge, but it is all worth it when the final "product" was in sight. It has been an interesting learning experience!

I would like to thank my supervisor professor Sigurd Skogestad and Ph.D. student Jens P. Strandberg for their guidance and support with the work. I also want to express my gratitude to post.doc. Eduardo Hori for showing me the inner workings of the Aspen Plus process modelling tool, and to Knut Arne R. Munkebye for his work with the gas chromatograph. Lastly, I would like to thank the 9 o'clock coffee crew and the exceptional Anne Øyen.

## Table Of Contents

1	Scope of work.....	1
2	Introduction .....	2
2.1	The Kaibel distillation column .....	2
3	General Distillation Theory.....	4
4	Operability of the Kaibel column .....	5
5	Experimental setup.....	6
6	Gas Chromatography .....	8
7	Modelling the column .....	10
8	Simulation results .....	13
8.1	Reflux .....	13
8.2	Vapour Split.....	17
8.3	Number of Equilibrium Stages .....	19
9	Experimental results.....	22
9.1	Calibration results .....	22
9.2	Verification of the calibration.....	22
10	Discussion of the results.....	24
10.1	Simulations of the Kaibel distillation column .....	24
10.2	Evaluation of the simulations .....	25
10.3	Experimental results .....	26
10.4	Evaluation of the experiment.....	26
11	Conclusion.....	28
	Bibliography.....	29
	Appendix A – Standards for the GC.....	30
	Appendix B – Calibration results .....	31
	Appendix C – Software descriptions .....	32

## 1 Scope of work

A Kaibel distillation column is a fully thermally coupled column, capable of separating 4 products in a single shell. This offers the possibility of reduced energy consumption and decreased investment costs compared to a conventional arrangement with 3 columns in series. However, due to its integrated nature, control and optimization of the column is difficult.

A possible solution is to control the column through the use of temperature sensors distributed in the column. By selecting the right sensors, the column can operate close to optimality, even in the presence of a disturbance. This is known as self-optimising control [Skogestad and Postlethwaite, 2005].

The aim of this thesis is to investigate the effect of different parameters on the optimal operation and the corresponding temperature profile of the column. Reflux rate and number of stages are examples of such variables.

Through simulations, optimal profiles and the corresponding optimal control variables can be found. Experiments can then be carried out, where the column is run at the optimal values from the simulations. The results of the experiments can be compared with the simulation results.

## 2 Introduction

In distillation, components are separated because of a difference in volatilities. Normally, one column is needed to separate a stream in two fractions; a distillate and a bottoms stream. This means separating a multicomponent mixture of 4 components would require 3 columns.

### 2.1 The Kaibel distillation column

The Kaibel column, introduced by Gerd Kaibel at BASF in 1987, separates four products in a single column shell with a single reboiler. The column offers large savings in energy and investment costs compared to the conventional sequential distillation arrangement for multicomponent systems. A similar sequential distillation setup would require three columns to separate four components. Hence, it also has the potential of saving space. Savings of 35 %, 25 % and 40 % for operating cost, investment cost and plot space respectively, has been reported [Wenzel and Röhm, 2003].

The Kaibel column is an extension of the Petlyuk column [Petlyuk *et al.*, 1965], and both the Petlyuk and the similar dividing wall column (DWC) [Wright, 1949] have been extensively investigated.

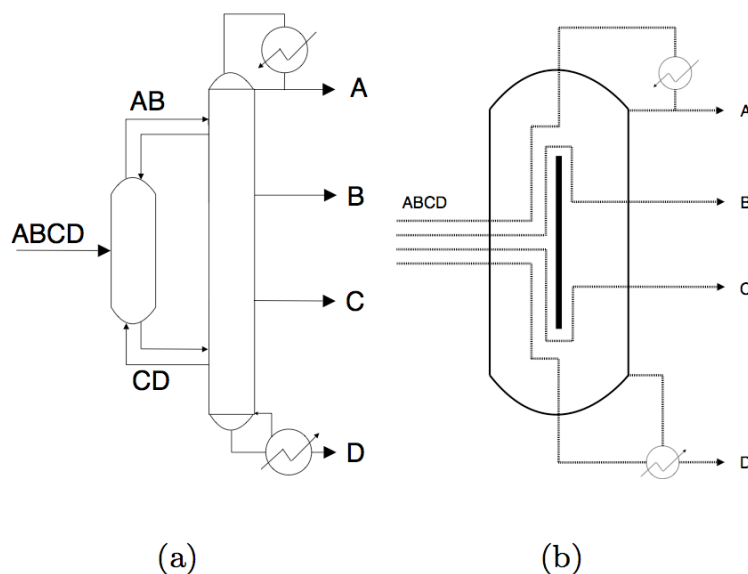


**Figure 2-1: Kaibel Column with a) a prefractionator arrangement, b) a one-shell arrangement.**

Figure 2-1 shows the Kaibel distillation column with a prefractionator arrangement and with an equivalent one-shell arrangement. Ideally, the aim of the prefractionator in (a), or the left side of the wall in (b), is to obtain the AB/CD split. The A/B and C/D separations will then occur at the top and bottom of the dividing wall in (b), or

upon entering the main column in (a). The arrows in the figure indicate this, and this is known as the components optimal travel paths.

### 3 General Distillation Theory

Distillation is a vapour-liquid separation process. A multicomponent mixture is separated due to a difference in volatility, and hence a distribution of the components between the vapour and the liquid phase. The vapour phase is created from the liquid phase by vaporization at the boiling point. The ease of a distillation separation process depends on the volatility of the components and in turn their boiling points.

The driving force behind the separation is energy, supplied to the column through the reboiler. Continuous distillation is a multistage separation process. The vapour and liquid phases come in contact with each other at each stage and a re-distribution of the components towards equilibrium occurs. This is shown in Figure 3-1. With sufficient contact time equilibrium is reached. However, this is seldom the case in real distillations. Nevertheless, the equilibrium model serves as a good conceptual model for understanding the physics of the distillation separation process.

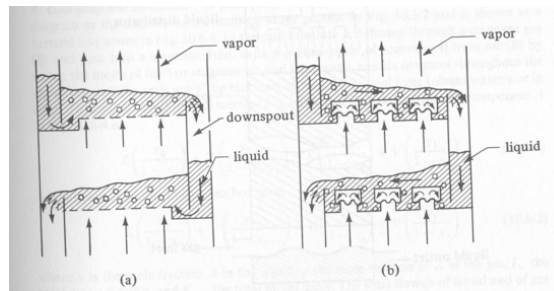


**Figure 3-1: Distillation separation. Component diffusion occurs across phase boundaries on trays. Figure (a) shows a tray from a sieve-tray tower, while (b) shows a bubble-cap tower tray [Geankoplis, 1993].**



## 4 Operability of the Kaibel column

It is desirable to operate the distillation process at an optimum. As this is a separation process, the optimum is associated with purity of product streams, while at the same time minimizing the energy consumption. Measuring the compositions on-line for a continuous process is hard and time consuming. Therefore, one seeks to identify other variables that allow for easier optimization.

For a chemical process it is often economically imperative to stay close to the optimum. The optimum is often dependent on process conditions, and may be affected due to disturbances. As production is economically motivated, the optimisation is essential. This situation can be expressed mathematically as:

$$L = J(u, d) - J^*(d) \quad (4.1)$$

where  $L$  is the loss resulting from a disturbance,  $J(u, d)$  is an objective function describing the operational objective at optimum, and  $J^*(d)$  is the optimum for a given disturbance.

According to Skogestad and Postlethwaite [Skogestad and Postlethwaite, 2005], one solution to achieve a minimal loss is through self-optimizing control:

*Self-optimising control is when we can achieve an acceptable loss with constant set-point values for the controlled variables without the need to reoptimise when disturbances occur.*

The singular value method [Halvorsen *et al.*, 2003] can be used to select the controlled variables. This method can roughly be summarised in the following steps [Strandberg and Skogestad, 2006]:

1. Obtain a linear model  $G$  from inputs  $u$  to the candidate controlled variables  $y$ .
2. Scale the inputs  $u$  such that the effect of each input is the same on the objective function.
3. Obtain the scaled gain  $G_s$  of the model by scaling the outputs using sum of their optimal range and their implementation error (“span”).
4. Select controlled variables that maximize the minimum singular value  $\underline{\sigma}$  of the scaled gain matrix  $G_s$  from  $u$  to  $y$ .

Hence, one seeks to identify a control structure that will give satisfactory optimality through a constant set-point policy. For the Kaibel column setup, this has been investigated elsewhere [Strandberg and Skogestad, 2006], and will not be given much attention here.

## 5 Experimental setup

A laboratory column has been built at the Norwegian University of Science and Technology (NTNU), for the purpose of investigating the controllability of the column. The arrangement is a two-shell implementation (Figure 2-1(a)), but it is equivalent to a divided wall column with no heat transfer across the partitioning wall. The column is made up of sections of vacuum-jacketed glass of internal diameter 50 mm. Further insulation is unnecessary because of the vacuum-jacket. Heat is supplied through a kettle reboiler with a capacity of 3 kW. Preheating of the feed is also available.

Figure 5-1 shows the experimental setup. The column consists of 7 sections of equilibrium stages. Sections 1 and 2 make up the prefractionator, having 7 and 9 equilibrium stages respectively. Sections 3 through 7 make up the main column. Sections 3, 5 and 6 each have 6 equilibrium stages, while sections 4 and 7 each have 4 equilibrium stages.

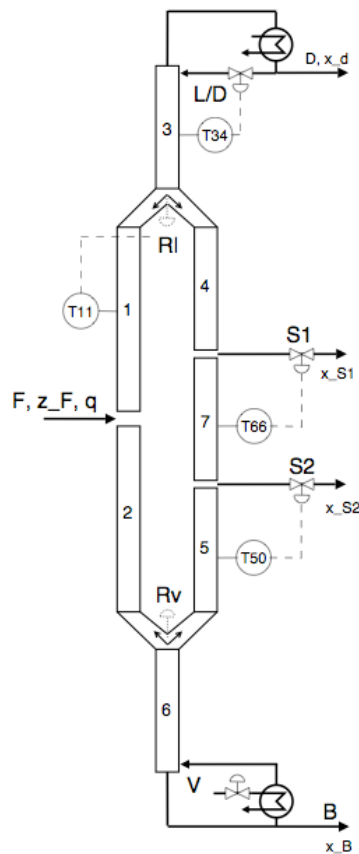


**Figure 5-1: The experimental Kaibel column setup, also showing the control structure [Strandberg and Skogestad, 2006].**

Solenoid operated swinging funnels, built into the glass sections, control the product streams (except bottom stream). The liquid split  $R_l$  between the prefractionator and main column is also set with a funnel. A device is implemented to control the vapour split  $R_v$ , however this currently only offers manual adjustment.

A total of 24 temperature sensors are distributed inside the column sections. These make up the majority of the on-line measurements. The goal is to use these temperature sensors to estimate the composition profile of the column and hence the purity of the product streams.

Product samples are analyzed off-line with a gas chromatograph to validate the estimates and help in fine-tuning the process.

The column is run with a mixture of alcohols, as shown in Table 5-1 below, and with partial preheating ( $q = 0,48$ ). The table also shows the boiling points of the components.

**Table 5-1: Feed stream composition and respective boiling points [Aylward and Findlay, 1998].**

	Amount	Boiling point
Methanol	18%	64,7 °C
Ethanol	33%	78,3 °C
1-Propanol	37%	97,2 °C
n-Butanol	12%	117,7 °C

The positioning of the temperature sensors and the control structure has been investigated elsewhere [Strandberg and Skogestad, 2006]. The best candidate structure is shown in Figure 5-1.

## 6 Gas Chromatography

Samples taken from the column's product streams will be analysed off-line with a gas chromatograph. In gas chromatography, components are separated due to chemical differences that lead to different transport rates through a capillary column. A typical gas chromatography setup is shown in Figure 6-1.

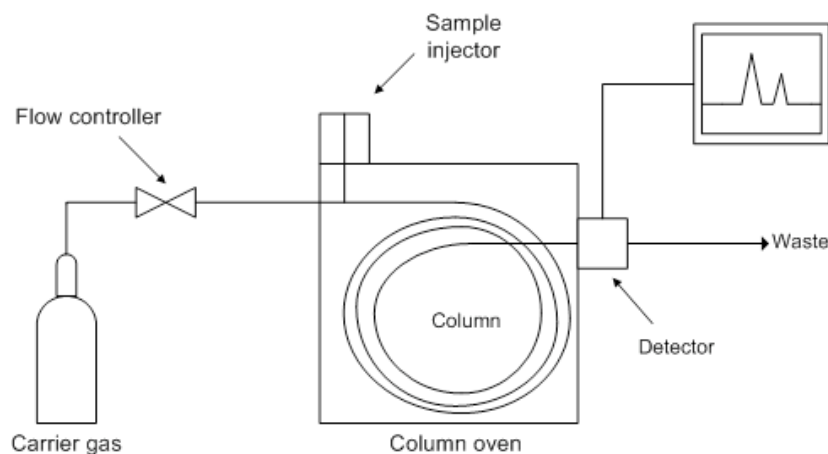


**Figure 6-1: A typical gas chromatograph setup.**

To determine the composition of the tested sample, calibration is needed. By knowing the amount and concentration of an internal standard, one can identify the amount of other substances through a comparison of the area trapped by the sample's detector signal. By first running a known sample, a relationship, known as the response factor ( $RF$ ), can be established. This is found by equation (6.1) where  $m_i$  is the mass of component  $i$  in the sample,  $m_{std}$  is the mass of the internal standard in the sample,  $A_{std}$  and  $A_i$  are the areas captured by the signal peaks of the internal standard and sample  $i$  respectively. 1-Pentanol is used as internal standard.

$$RF = \frac{m_i}{m_{std}} \cdot \frac{A_{std}}{A_i} \quad (6.1)$$

Furthermore, when an unknown sample is tested, the equation above is rearranged to solve for the desired mass of sample  $i$ . The areas of the peaks are found by numerical integration.

A Chromopack CP9000 Gas Chromatograph is available for sample analysis. The chromatograph has a Flame Ionisation Detector (FID) and an on-column injector. The column used is a 10 meter long fused silica capillary column with inner diameter 0,53 mm. To avoid overloading of the GC column and the detector, a dilution ratio of 1:1000 of sample and solvent is used [Wittgens, 1999]. As the FID does not detect water, it is natural to use water as the solvent. The installation parameters of the GC are shown in Table 6-1.

**Table 6-1: Gas Chromatograph operating parameters.**

	Gas	Flows [ml min <sup>-1</sup> ]	Inlet Pressure [kPa]
Carrier gas	Nitrogen	3	200
Makeup gas	Nitrogen	27	200
Detector	Air	200	200
	Hydrogen	30	200

Both air and hydrogen are used for detection purposes. The gases used are analysis quality pure. With the components used in the distillation experiment in mind, a temperature program has been designed. Operation parameters for the analysis of methanol, ethanol, propanol, butanol and pentanol samples, are shown in Table 6-2 [Wittgens, 1999]. The temperatures and temperature program are essential in achieving a proper separation of the compounds in the capillary column.

**Table 6-2: Operation parameters for the designed GC program.**

	Temperature
Temperature injection port	240 °C
Temperature detector	250 °C
Oven temperature	40 °C for 0,5 min followed by a 10 °C/min ramp increase to 150 °C
Final oven temperature	150 °C for 10 min to clean/regenerate column

As mentioned earlier, the gas chromatograph needs calibration. A number of calibration samples are prepared. These samples are made to resemble the expected compositions of the product streams. The standard samples are given further attention in Appendix-A. The calibration is performed on mass basis, rather than mole basis.

After finding the response factors, the actual experiment samples can be analysed.

- Firstly, the total weight of the sample is recorded.
- Next, an amount (around 1-2 weight %) of the internal standard is added to the experiment sample.
- A 10 µL sample is extracted with a vial from the experiment sample, placed in a new container, and diluted with 5 ml of water.
- Now, less than 1 µL of the diluted sample is injected into the injection port of the GC. The sample should be injected as a plug. Rapid and consistent injection is necessary to achieve acceptable precision and good separation of the peaks.
- The chromatograph's program and the connected recording computer are started.
- A few parallels should be run to achieve an average, and ensure consistency.

The GC-signal is fed into Labview in the connected computer. After the analysis is complete, the signal plot is analysed with Matlab. The start and end points of the peaks are determined. With this information and a numerical integration routine programmed in Matlab, the areas of the peaks are determined. By the aid of equation (6.1), the composition of the sample is found.

## 7 Modelling the column

The Kaibel column was modelled in the process simulator Aspen Plus. It was modelled to resemble the laboratory setup, hence a prefractionator arrangement was chosen. The model was built with the same specifications as described in the experimental section. Figure 7-1 shows the Aspen Plus model.

An important goal for the modelling is to achieve the right separations at the right positions in the column. The arrows in Figure 2-1 b) shows the optimal travel paths of the different components. It is important for optimal operation that the AB/CD split occurs in the prefractionator. If component C travels over the top, or component B travels under, a penalty will be imposed in the form of extra energy consumption, a reduced degree of separation, or both.

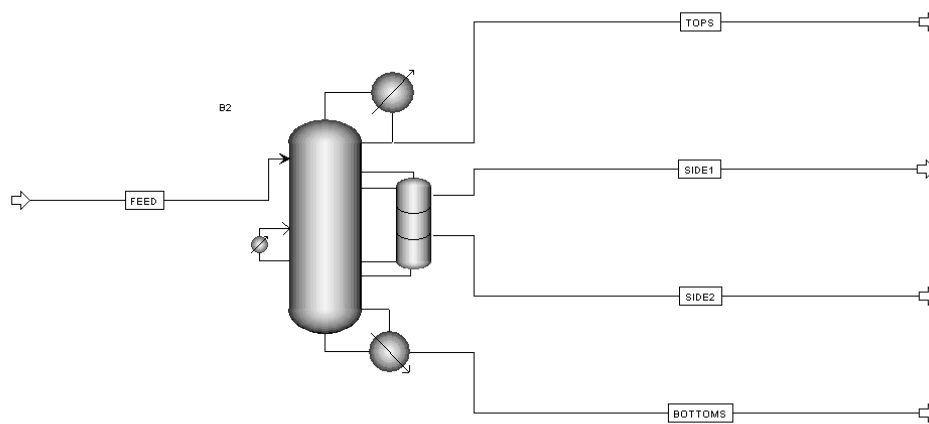


**Figure 7-1: The modelling setup in Aspen Plus.**

There are 6 steady-state degrees of freedom available for control and optimisation of the column. The set of control variables chosen are the three product streams; the distillate stream ( $D$ ), side stream 1 ( $S1$ ) and side stream 2 ( $S2$ ). Additionally, the liquid ( $R_l$ ) and vapour ( $R_v$ ) splits are controlled, as well as the reflux rate ( $L/D$ ). Initially, the reflux rate will be varied. The controlled variables were defined as described in Table 7-1.

**Table 7-1: The controlled variables.**

$$D = z_A \cdot F$$

$$S1 = z_B \cdot F$$

$$S2 = z_C \cdot F$$

$$L/D = 12$$

$$R_v = 0,5$$

$R_l$  = Set to optimise the prefractionator  
B/C component split

Where  $z_i$  is the mole fraction of component  $i$  in the feedstream  $F$ . The reflux ratio ( $L/D$ ) is initially set to 12, however this will be varied through the simulations. The same is the case for the vapour split ( $R_v$ ). The liquid split  $R_l$  is set to obtain the optimal B/C component split in the prefractionator. Both the vapour split ( $R_v$ ) and the liquid split ( $R_l$ ) is defined as the fraction of the rising vapour stream and the downcoming liquid stream respectively being sent to the prefractionator. Hence, a larger value, means more is being sent to the prefractionator, and less to the main column. It is interesting to investigate the effect of the reflux, the vapour split and the number of stages on the degree of separation, the heat duty and the optimal temperature profile.

The feed stream composition for the simulations are the same as that defined in Table 5-1. The other feed stream specifications are listed in Table 7-2.

**Table 7-2: Feed stream conditions.**

Temperature	345	[K]
Pressure	1,2	[atm]
Flow rate	100	[kmol h <sup>-1</sup> ]

Three different column sizes are investigated. Starting with the base case of 42 stages, which is the same as the laboratory column. The other 2 columns simulated have the same general shape, however the number of stages differ. Table 7-3 shows the column arrangements for the different sizes. The section numbers refer to the sections in Figure 5-1. As of now, the columns will be referred to by their total number of equilibrium stages. When it comes to the numbering of the equilibrium stages in the column, the top stage is number one, while the bottom stage is the last stage (highest number).

**Table 7-3: Table showing the different columns sizes.**

Section Number	Equilibrium Stages		
	42	50	59
1	7	8	9
2	9	11	14
3	6	7	8
4	4	5	5
5	6	7	8
6	6	7	8
7	4	5	7

In Aspen Plus, the user defines a property set to use. According to the Aspen Plus help function, this is “*a collection of thermodynamic, transport and other properties*”. The property set used in the simulations is the Wilson property set.

As mentioned earlier, it is important to obtain a good AB/CD split in the prefractionator. The liquid split ( $R_l$ ) at the top of the column is used to achieve this. The Aspen Plus model is put together by two columns as shown in Figure 7-1. Comparing this figure to the arrangement shown in Figure 5-1, there are a few differences. These do not impact the simulation results, but are needed for the

modelling. In effect, there are 2 columns in the Aspen Plus model. Column 1 makes up sections 1,2,3 and 6 of Figure 5-1, while column 2 is makes up sections 4,5 and 7 of the same figure. The two columns are interlinked by connect streams between the columns in such a way that the shape of Figure 5-1 is achieved. These connect streams are then used to manipulate the vapour and liquid splits.

The AB/CD split was optimised by setting the fraction of component B at the bottom of the prefractionator equal to the fraction of component C at the top of the prefractionator. That is, for the case of 42 stages:

$$x_{B,22} = x_{C,7} \quad (7.1)$$

It is important to notice that the stage numbering refers to the modelling described earlier. I.e. stage 22 is at the bottom of the prefractionator, and stage 7 is at the top of the prefractionator. In effect, what one seeks to achieve by optimising the prefractionator split, is to maximize the products in the side product streams.

The vapour split at the bottom of the column is implemented by specifying volume flowratios for some stages in the column. Figure 7-2 shows the setup. The connect stream is used to set the ratio of the vapour streams of stage n-1 relative to the vapour stream at stage n+1 to the desired  $R_V$  value. That is:

$$R_V = \frac{V_{n-1}}{V_{n+1}} \quad (7.2)$$

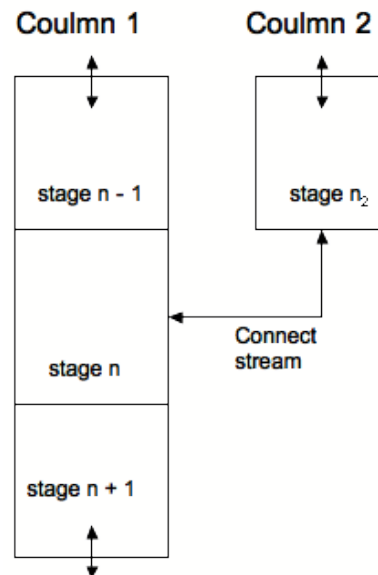


**Figure 7-2: Figure showing the columns and connect stream arrangement used to set the vapour split.**

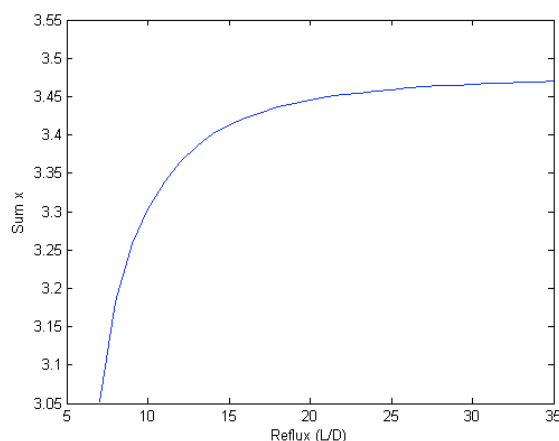


## 8 Simulation results

A number of simulations were carried out to investigate the temperature profile associated with a given setup. Certain other key parameters are also of interest, such as the sum of the component product fractions in the respective product streams, also called the degree of separation. The simulations were carried out in Aspen Plus with the parameters given in the modelling section of this thesis. Aspen Plus' sensitivity function was used to investigate the column's dependence on the given variable. A copy of the simulation raw data can be found on the cd following this thesis.

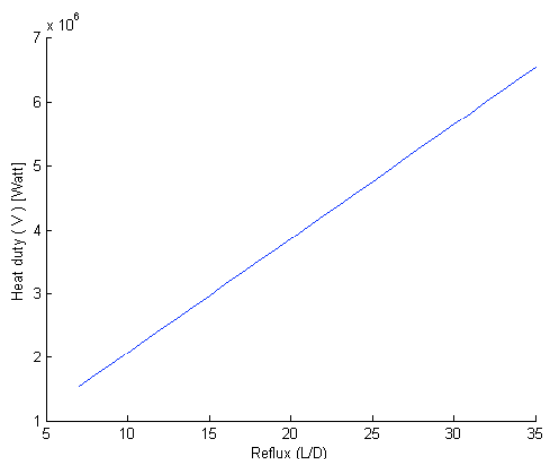
### 8.1 Reflux

The base case defined in Table 7-1 has a reflux of 12. In this section the impact of the reflux on the column is investigated. The reflux was increased from 7 to 35 with unit increments. The other variables were kept constant at the values given in Table 7-1. The degree of separation, is shown in Figure 8-1.



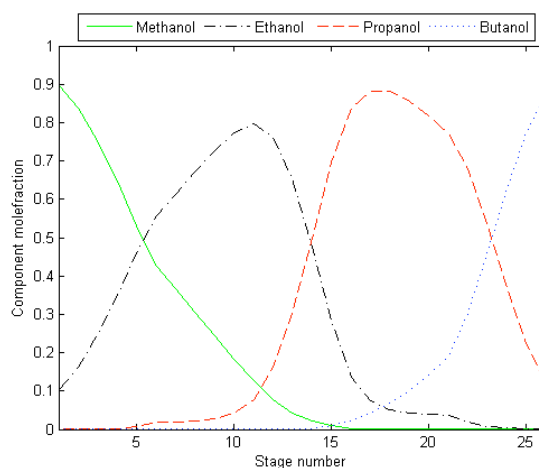
**Figure 8-1: A plot of reflux (L/D) against the degree of separation.**

It is evident that the effect of increasing the reflux is significant on the separation of the components. However, this effect is decreasing with the amount of reflux. Figure 8-2 shows the relationship between the reflux and the heat duty in the reboiler at the bottom of the column. This relationship is linear and increases with the reflux. Hence, from Figure 8-1 and Figure 8-2 one can conclude that the increased separation, shown in the first figure, comes at an increasingly higher price.



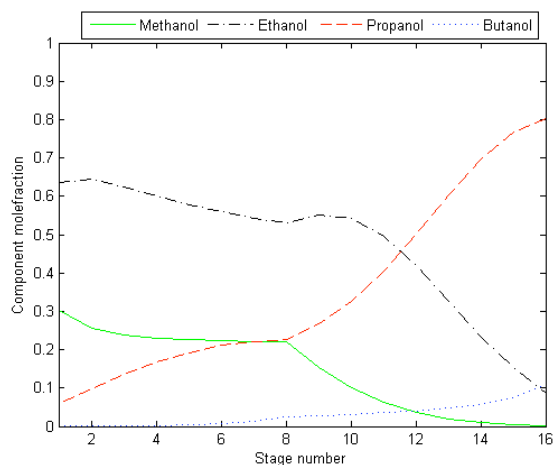
**Figure 8-2: A plot of reflux against the heat duty in the kettle reboiler at the bottom of the column.**

Figure 8-3 shows the composition profile of the main column for a reflux of 12.



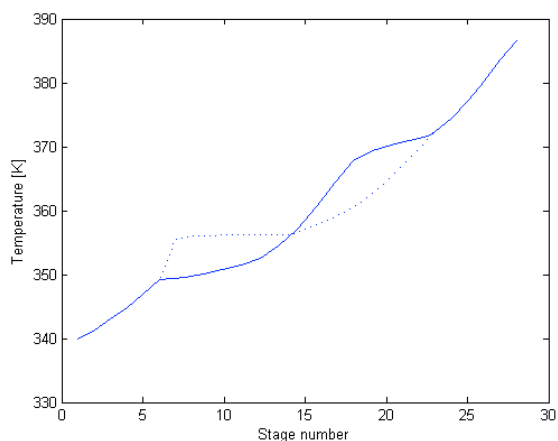
**Figure 8-3: The composition profile of the main column (not showing the prefractionator). This plot is for a reflux of 12.**

Figure 8-4 shows the composition profile in the prefractionator for the same simulation. The feed is introduced between stages 7 and 8. Looking at the compositions at the extremes, i.e. stages 1 and 16, it is clear that the prefractionator split is working reasonably well. The composition of ethanol at the bottom stage is almost the same as the concentration of propanol on the top stage. The same is shown by Figure 8-3, but this figure is not as easy to interpret. It is important to notice that the stages in Figure 8-4 refer to the prefractionator alone.



**Figure 8-4: The composition profile of the prefractionator (not showing the main column). This plot is for a reflux of 12.**

Looking at the temperature profile of the column, the difference between the prefractionator and the main column decreases with the reflux. Figure 8-5 shows the temperature profile for the column with a reflux of 7.



**Figure 8-5: Temperature profile in the column with a reflux of 7. The solid line shows the main column, while the dotted line shows the prefractionator.**

The feed is introduced at stage 15, and explains the flat prefractionator profile around this stage. With increasing reflux, the effect of the feedstream decreases, because the feed rate relative to the column holdup is reduced. Figure 8-6 shows the profile for the base case of a reflux of 12. The profile has levelled out compared to the profile representing a reflux of 7.

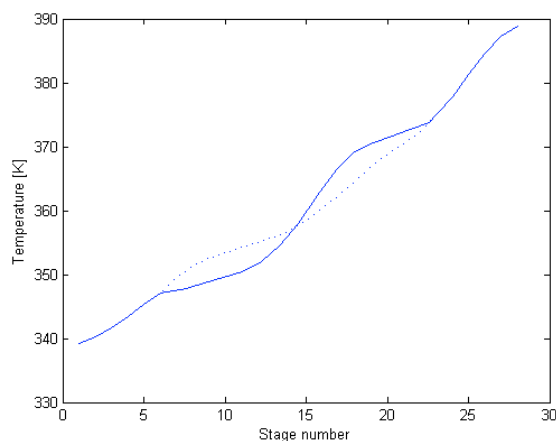


**Figure 8-6: Temperature profile in the column with a reflux of 12. The solid line shows the main column, while the dotted line shows the prefractionator.**

The unrealistic case of a reflux of 34 strengthens this statement further. This case is unrealistic because the increase in purity of the products can not be justified by the increased energy needed for the separation. Figure 8-7 shows the profile for the column operated with a reflux of 34.

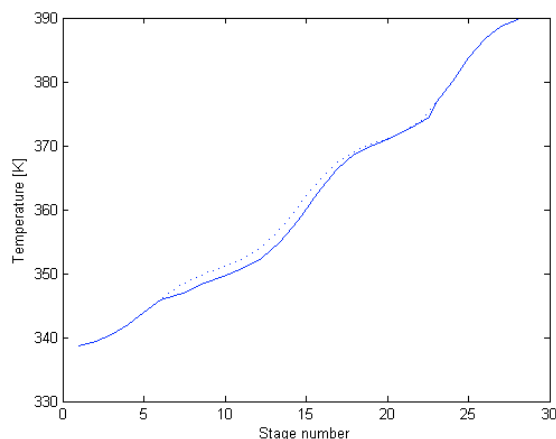


**Figure 8-7: Temperature profile in the column with a reflux (L/D) of 34. The solid line shows the main column, while the dotted line shows the prefractionator.**

With a reflux of 34, the main column and the prefractionator are almost equal through most of the column.

A comparison of the temperature profiles in the main column is shown in Figure 8-8. The operating temperature range of the column expands and the profile straightens out as the reflux increases.

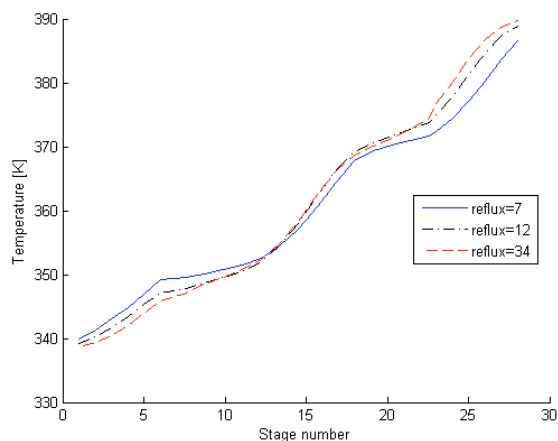


**Figure 8-8: Temperature profile of the main column for three different refluxes. The prefractionator is left out of the diagram to ease the interpretation.**

## 8.2 Vapour Split

The vapour split ( $R_V$ ) sets the distribution of the rising vapour between the prefractionator and the column.  $R_V$  is the fraction of the rising vapour stream that is being sent to the prefractionator. A larger value means more is being sent to the prefractionator, and less to the main column. The simulations were carried out with the controlled variables defined in Table 7-1. The vapour split was varied from 0,2 to 0,8 with a mix of 0,5 and 1,0 increments. Figure 8-9 shows a plot of the vapour split against the degree of separation.

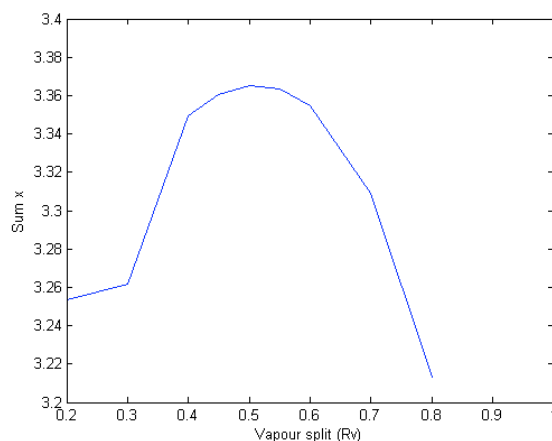


**Figure 8-9: A plot of vapour split against the degree of separation.**

The optimal solution seems to be with an even split between the prefractionator and the main column, that is  $R_V=0,5$ . Figure 8-10 shows a plot of the vapour split against the heat duty of the kettle reboiler. Even though the optimal split with respect to the separation of the products is not the minimum on the energy curve, it is probably worth the extra spending of energy.

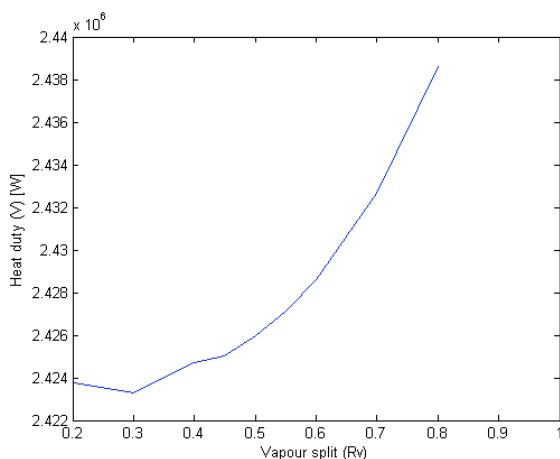


**Figure 8-10: A plot of vapour split against the heat duty in the kettle reboiler at the bottom of the column.**

Looking at the temperature profiles associated with the vapour splits, the same ideas can be applied as with increasing reflux. Figure 8-11 shows the temperature profile for a vapour split of 0,3. A vapour split of 0,3 means that 30 % of the rising vapour stream is sent to the prefractionator. The remaining 70 % goes to the main column. In effect, this leads to a lower vapour stream in the prefractionator, and hence the feed stream has a larger impact on the column's profile. The product streams have a lesser effect on the main column's profile as opposed to the case of a 50 % vapour split, as shown in Figure 8-6.

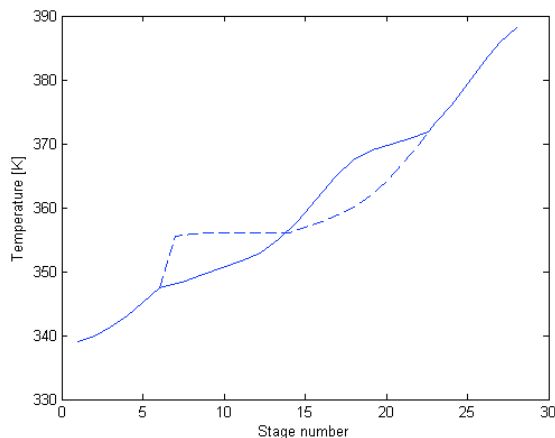


**Figure 8-11: Temperature profile in the column with a vapour split of 0,3. The solid line shows the main column, while the dotted line shows the prefractionator.**

This statement is further strengthened by Figure 8-12, which shows the temperature profile of a vapour split of 0,7. This means 70 % of the rising vapour stream is sent to the prefractionator, while the remaining 30 % goes to the main column. The effect of the feed stream is reduced due to the larger volume flow in the prefractionator. The main column on the other hand, is largely affected because of the decreased volume flow in this section of the column.

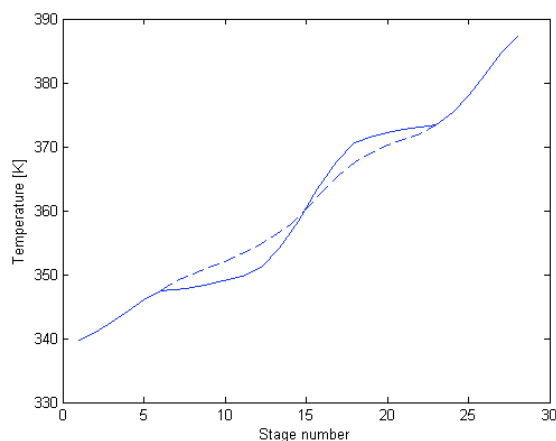
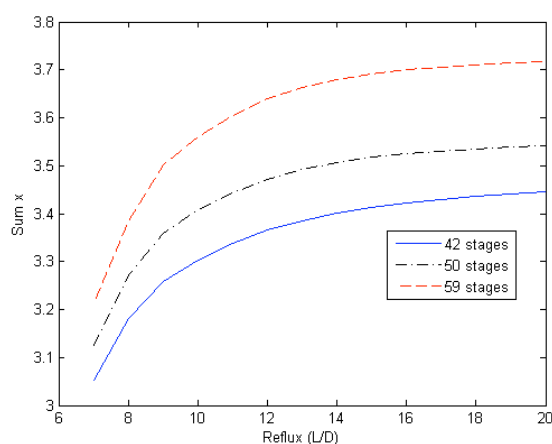


**Figure 8-12: Temperature profile in the column with a vapour split of 0,7. The solid line shows the main column, while the dotted line shows the prefractionator.**

### 8.3 Number of Equilibrium Stages

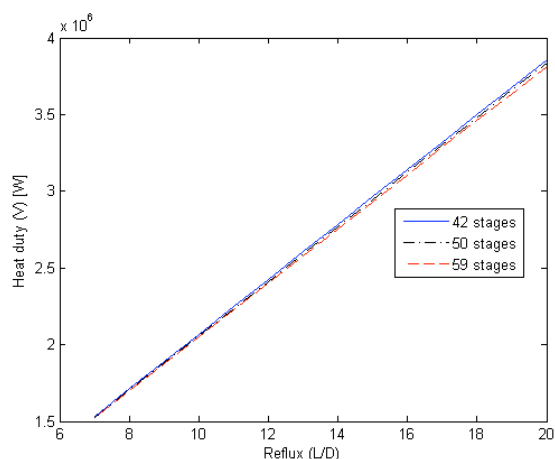
The degree of separation a distillation column can achieve is highly dependent on the number of equilibrium stages in the column. Initially, a column identical to the lab scale column at NTNU has been considered. It is also interesting to look at the effect of increasing the number of stages. The added equilibrium stages are distributed evenly to the different sections of the column, hence keeping the overall shape constant. The column sizes can be seen in Table 7-3.

Figure 8-13 shows the effect of added equilibrium stages on the separation performance of the column. The number of stages refers to the total number of stages in the column. That is the prefractionator plus the main column.



**Figure 8-13: A plot of reflux against the degree of separation.**

Looking at the heat duty associated with the given refluxes for the different column sizes as shown in Figure 8-14, it can be seen that the heat duty is nearly independent of the number of stages.



**Figure 8-14: Plot of reflux against the heat duty in the kettle reboiler.**

From this, one can deduce that to achieve a certain degree of separation, one can either do this through increasing the number of stages, or by increasing the reflux. Adding more stages will bring up the investment cost, while escalating the reflux will increase the operational costs.

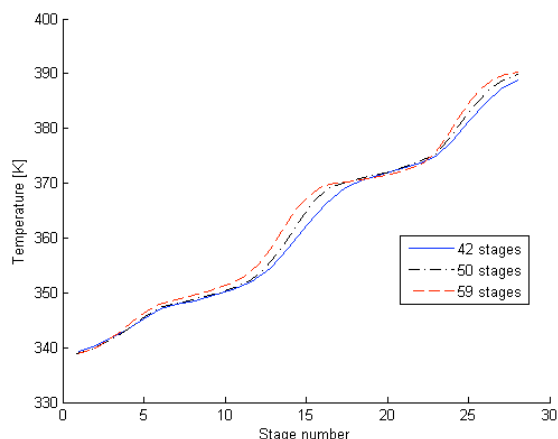


**Figure 8-15: Temperature profile in the main column with a reflux of 12 and a vapour split of 0.5. The plot shows three different column sizes. The stage numbering refers to the case of 42 stages.**

Figure 8-15 shows the temperature profiles of the column for the three different sizes. The stage numbering has been modified to allow for easy comparison of the different cases. The numbering refers to the base case of 42 stages. Only the main column is shown in the plot. The temperature profile itself, seems to level out around the boiling points of the components when more stages are added. Looking at the curve for the case of 59 stages, the profile is almost level around stages 17-18.

Figure 8-16 shows the composition profile in the column for the three different column sizes. Again, the increased number of stages result in a higher degree of separation. Note also the success of the prefractionator split as mentioned earlier.



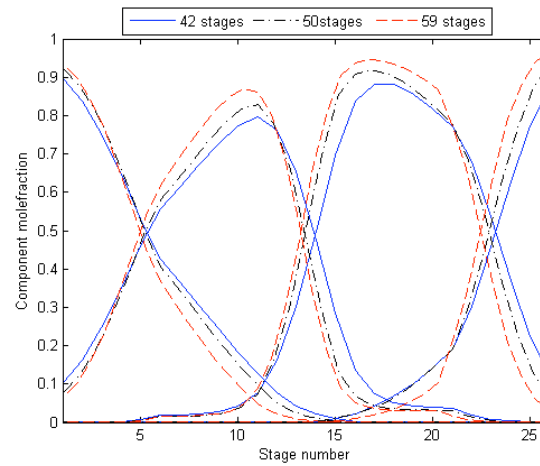


**Figure 8-16: The composition profile in the main column for the three different column sizes. All components for a given size are depicted by the same colour. The stages refer to the case of 42 stages.**

## 9 Experimental results

The lab scale column was used to run experiments with the optimal temperature profiles found through the simulations. The gas chromatograph was used to evaluate the product stream samples and determine the composition of these. First, the gas chromatograph was calibrated, and the response factors of the different components were found. Then, by using these response factors, the composition of the experimental samples could be found. All the raw data from these analyses can be found on the cd at the back of this thesis.

### 9.1 Calibration results

Initially, the calibration was performed using the method of Wittgens' [Wittgens, 1999]. This method finds the response factors by assuming they are nearly independent of concentration. According to Wittgens, when comparing two samples with main components of mole fraction 0,85 and 0,98, the "variations of the relative response factors are rather limited"(p. 152). Using this method and formula (6.1), a set of response factors were found. These are shown in Table 9-1. A standard deviation analysis was also performed and is shown in the same table.

**Table 9-1: Response factors from the calibration of the GC.**

	Methanol	Ethanol	Propanol	Butanol
$RF$	3,270	2,228	1,709	1,355
$\sigma_{RF}$	0,721	0,188	0,135	0,100

The standard deviations shows inaccuracies of 22, 8, 8 and 7 percent. After evaluating these results, it was decided to perform further calibration. This involved making new calibration samples, with concentrations over a wider range. Analysis of the new calibration sample, yielded the results shown in Table 9-2. The standard deviation analysis is shown in the same table. The standard deviations show inaccuracies of 60, 67, 25 and 33 percent respectively. The results given in the table are actually an average of the different concentrations. Nevertheless, the results in the table are very much different from the results found by Wittgens' method. A proper results table for the performed analyses are given in Appendix-B.

**Table 9-2: Response factors from the calibration of the GC.**

	Methanol	Ethanol	Propanol	Butanol
$RF$	7,119	4,153	2,564	2,097
$\sigma_{RF}$	4,223	2,777	0,639	0,700

### 9.2 Verification of the calibration

To ensure that the calibration was performed correctly, and would yield correct results, a control sample was made. With this sample, the aim was to find the

concentration by using the response factors found during the calibration. The exact concentration was recorded when making the sample. The results in %, of the unknown control sample are shown in Table 9-3. The table also shows the actual composition, and the standard deviation of the unknown test results.

**Table 9-3: Results of the unknown control sample.**

	Methanol	Ethanol	Propanol	Butanol
Actual composition	8,43	79,01	11,52	1,04
Experimental composition	4,17	71,51	21,95	2,36
$\sigma_{Exp}$	0,22	1,99	2,19	0,12

The results of the control sample are clearly not very accurate. With a 50 % error at the extremes, the verification of the calibration can be considered a failure.

After considering the results of the control sample, and due to time considerations, it was decided to not go further with testing samples. There had also previously been some uncertainty about the accuracy and general health of the gas chromatograph in use.

## 10 Discussion of the results

The results have been commented on throughout the results section of this thesis, however they need a more thorough inspection. There are also certain aspects of the simulations and experimental work that have its limitations or that are possible sources of error.

### 10.1 Simulations of the Kaibel distillation column

The simulations established some well-known facts of multicomponent distillation theory, such as the effect of reflux and number of stages on the degree of separation. The effect of increasing the reflux or the number of stages only serves to validate the model. Nevertheless, these results can aid in understanding the inner workings of the column.

Figure 8-1 and Figure 8-13 supports the statement of the reflux's impact on the degree of separation. Figure 8-13 also proves that increasing the number of stages improves the column's performance. With respect to reflux, this is explained by the stabilisation of the temperature profile due to the increased volume flow. This will be given more attention later. By increasing the number of equilibrium stages in the column, there are more plates for the gas and liquid to interact at, and hence a higher degree of separation is achieved.

Figure 8-2 and Figure 8-14 shows that there exists a linear relation between the reflux and the heat duty associated with a given reflux. This is not a surprising fact, as by increasing the reflux, a larger amount has to be vaporised. This amount is of course independent of the column size. The dependence is on the steady state mass balance, and hence the heat duty is nearly constant for all number of stages.

Combining the two results above, it is evident that there are two ways of improving the column's performance. Through a higher reflux, or by adding more equilibrium stages. The first suggestion results in an increased operational cost due to the higher heat duty. While, on the other hand, the latter suggestion results in an increased investment cost because of the expenditure on the extra number of equilibrium stages.

Now, turning the attention to the effect of the vapour split.  $R_v$  changes the operation of the column because it changes the vapour flow, and in turn the effect the feed and product streams impose on the column. The optimal value for the vapour split seems to be around the 50/50 even split between the prefractionator and the main column. Looking at the associated heat duty in the reboiler, the minimum energy consumption is not at the optimal vapour split with respect to the degree of separation. Furthermore, it is worthwhile noticing that increasing the vapour split past 0,5 will have negative effects on both the total degree of separation and the heat duty.

Although it is a good indicator to consider the total degree of separation, i.e. the sum of the component product mole fractions in the respective product streams, it may be desirable to produce a certain component at a higher purity than others. From Figure

8-3 and Figure 8-16 it is clear that the products are not produced in equal purity. Figure 8-16 shows that increasing the number of equilibrium stages evens this out. Furthermore, even though not investigated here, the vapour split and the liquid split may be used to alter the distribution of the product purities, and hence prioritise a certain stream or component.

Looking at the temperature profiles for the different arrangements, it becomes clear that this is altered depending on the vapour and liquid streams in the column. The feed and product streams affect the column's temperature profile, as heat follows these streams. The changes in the temperature profile from changing variables, can be explained from the column's hold-up and flowrates relative to the feed and product streams. For example considering Figure 8-5 and Figure 8-7, with refluxes of 7 and 34 respectively, it is clear that the profile straightens out and the "corners" in the first figure disappears. This is due to the increased hold-up resulting from a higher reflux, and hence the lessened effect of the feed and product streams. Considering the vapour split results, Figure 8-11 with  $R_v=0,3$ , shows a straightened profile in the main column, and a more cornered profile in the prefractionator. This is due to the imbalanced vapour flow created by the  $R_v$  setting. The main column is straightened because the feed flowrate is reduced relative to the vapour and liquid flowrates in the main column. In Figure 8-12, with a vapour split of 0,7, the situation is reversed, and the larger vapour flow is in the prefractionator. This leads to the straightened prefractionator profile. The reduced vapour flow in the main column leads to the sharper, more cornered profile. Hence the feed and product streams relative to the hold-up in the column determine the temperature profile.

## **10.2 Evaluation of the simulations**

A large obstacle in the simulation of the column was to achieve the optimal prefractionator split. Several attempts were made at finding the best specification set to achieve the optimal split. The best solution was determined to be the method described in the modelling section of this thesis. That is, to use the liquid split to achieve an equal concentration between components B and C at the bottom and top of the prefractionator respectively. Although the numerical methods used by Aspen Plus did not fully converge to this specification, the results were reasonably good. A copy of the raw data from Aspen Plus is available on the cd following this report. Figure 8-4 shows the composition profile for the prefractionator with a reflux of 12. This figure supports the statement of a reasonably good split. By achieving this split, it also means the optimal travel paths for the components are more closely followed. These paths are shown in Figure 2-1 b).

Furthermore, the modelling of the vapour split does not exactly equal the real case. However, the model performs well enough, and one can not expect the experimental columns performance to do much better. Nevertheless, for the purposes of optimisation this could be improved.

The main goal of the simulation is to achieve the highest possible degree of separation the column can yield with the given parameters. This is called optimisation. The simulation software has a built in optimisation routine, however this proved to

perform worse than the prefractionator split specification used in this thesis. The optimisation routine was not rigorously tested though.

The split variables, both the vapour split ( $R_v$ ) and the liquid split ( $R_l$ ), are used to control the column and achieve the specifications. However, when performing analysis on one of the variables, the other might counteract the effect of the change. When performing the vapour split analysis, the liquid split was still set to obtain the desired prefractionator split. Hence this was in effect a free variable, and the value of it unknown. However, later a smaller, less thorough simulation was performed to check the dependence of this prefractionator split on the vapour split simulations. In this smaller simulation the prefractionator specification was removed, and the results showed little change compared to the main simulation with the split specified. Nevertheless, this ought to be given further attention.

### **10.3 Experimental results**

The experimental gas chromatograph results were meant to validate and confirm the results of the simulations. Unfortunately, the calibration of the GC proved difficult and inaccurate. Not many conclusions can be drawn from the results. An attempt at testing the accuracy was made, by running a known control sample, but the findings were very inaccurate when compared to the actual values. The results showed a too small concentration of the lighter components (methanol and ethanol) and a too high concentration of the heavier components (propanol and butanol). This can be due to the lighter components having a higher tendency to evaporate. However, then this should also have been the case during the calibration, and not just when running the control sample. A proper experimental validation of the simulation, by analysis of column samples, could not be achieved due to the inaccuracies of the gas chromatograph and due to time constraints.

### **10.4 Evaluation of the experiment**

There are numerous reasons why the experimental segment of this thesis did not go as planned. To start with, there had been doubts about the gas chromatographs accuracy and general health. Nevertheless, this should itself not be a reason for failing. Because of this previous lack of faith in the GC's performance, the capillary column was changed prior to starting the experiments. Therefore there are not any other results or calibrations to compare the results to.

Firstly, the sources of error in the procedure of the production of the samples will be considered. As mentioned earlier, a problem may be evaporation of the alcohols, especially the lightest component methanol. Although caution was taken when preparing the samples, a greater amount of methanol is likely to have evaporated, than the butanol. All samples were made by measuring the components out in order of boiling points. Starting with the least volatile pentanol (internal standard) and ending with the most volatile methanol.

Secondly, the sources of error in the gas chromatography procedure will be considered. As mentioned earlier, the separation is dependent on the temperature program used. A slower temperature rise from start to stop, should increase the separation and make the distinction of the different samples easier to determine. By decreasing the temperature rise, the sample run also takes a longer period of time. So a trade off between time and accuracy is needed. As many samples need to be analysed, there is a limit to the degree of separation that can be achieved by the temperature program. Ideally, a program with several different temperature ramp increases should be used. The GC used however, did not support this feature. The flow of gases is also a key factor in achieving a proper separation of the component peaks. However, these flows were recalibrated every now and then and should not be a source of error. Furthermore, it is important to inject the sample as a plug.

Thirdly, the error sources in the analysis of the signal profile from the detector will be considered. When analysing the results, it was hard to determine the start and finish values of each peak. Not all components were equally hard, but especially the heavier components that appear late in the profile were difficult because the baseline would not be consistent. For the lighter components, there were some separation problems. The methanol and ethanol peaks appear close in the signal profile, and so some runs gave a problem when it came to determination of the end of one and the start of the following component. Nevertheless, an educated guesstimate was performed in most cases. The importance of this error would however not be too large considering the total area of most of the peaks. Also, the error is likely to have been similar for all samples.

Lastly, considering the errors in the overall procedure. Initially, the runs were carried out with no overloads, and signal plots showing all component peaks completely. However, it was later learned that the conventional method of gas chromatography analysis is to only calculate the values of the impurities, leaving the main component to itself. The main component would later be calculated from the total mass balance, with the knowledge of the amount of impurities. The latter method of finding the composition is probably the better of the two. However, by overloading the column with the main component, it is likely to cause a terrible separation of especially the methanol and the ethanol peaks.

## 11 Conclusion

This thesis set out to study the behaviour of the Kaibel distillation column through simulations. Analysis of experimental results from a laboratory scale column was meant to support the results of the simulations.

The simulations were successfully completed in Aspen Plus. A few basic facts about distillation were established, such as the effect of increasing reflux on the degree of separation and the heat duty of the reboiler. This helped validate the model. Later, the effect of manipulation of the vapour split was investigated, and an attempted explanation was given. The vapour split had a large effect on the temperature profile in the column, while the changes in reflux and number of stages showed more moderate changes. A discussion of the problems concerning the model and the modelling was given.

A gas chromatograph was to be used to analyse the results from the experimental column. Firstly, the gas chromatograph was calibrated, finding the necessary response factors. Later, a control sample was analysed to check the accuracy of the chromatograph. The control sample analysis was determined to be too inaccurate, and the decision not to continue with further testing was made.



## Bibliography

[Aylward and Findlay, 1998]. Aylward, G., and Findlay, T., (1998). *SI Chemical Data*. 4<sup>th</sup> edition. Wiley & Sons.

[Geankoplis, 1993]. Geankoplis, C. J., (1993). *Transport Processes and Unit Operations*. Prentice-Hall.

[Petlyuk *et al.*, 1965]. Petlyuk, F. B., V. M. Platonov and D.M. Slavinskii (1965). Thermodynamically optimal method for separating multicomponent mixtures. *International Chemical Engineering* **5** (3), 555-561.

[Skogestad, 2000]. Skogestad, S. (2000). Plantwide control: the search for the self-optimizing control structure. *Journal of Process Control* **10**, 487-507. H2000-10.

[Skogestad and Postlethwaite, 2005]. Skogestad, S. and Postlethwaite, I. (2005). *Multivariable Feedback control: Analysis and design*. 2<sup>nd</sup>. Edition. Wiley & Sons.

[Strandberg and Skogestad, 2006]. Strandberg, J. and Skogestad, S. (2006). Stabilizing operation of a 4-product integrated Kaibel column. *ICHEME Symposium Series*, **152**, 638-647.

[Wenzel and Röhm, 2003]. Wenzel, S. and Röhm, H. (2003). Auslegung thermisch und stofflich gekoppelter destillationskolonnen mittels gesamtkostenoptimierung. *Chemie Ingenieur Technik*, 75:534-540.

[Wittgens, 1999]. Wittgens, B. (1999). Ph.D thesis: Experimental Verification of Dynamic Operation of Continuous and Multivessel Batch Distillation. NTNU Trondheim.

[Wright, 1949]. Wright, R.O. (1949), Fractionation apparatus. *US Patent No.2471134*.

## Appendix A – Standards for the GC

The standard samples for calibration of the gas chromatograph were created by making solutions that resembled the expected compositions of the product streams. The compositions of the first set of calibration samples are given in table A-1. These were the samples used in the Wittgens approach [Wittgens, 1999].

**Table A-1: The composition of the calibration samples.**

	Amount
Main component	50 ml
Each impurity	2 ml
Internal standard	0,5 gr.

The second set of calibration samples were planned with a completely different approach. These are shown in table A-2. Additionally, about 1,5 wt% of the internal standard (pentanol) was added to each sample. The first letter of each sample name denotes the product stream that it is intended to resemble.

**Table A-2: The composition of the calibration samples.**

	Methanol [%]	Ethanol [%]	Propanol [%]	Butanol [%]
D-1	95	5	-	-
D-2	90	9	1	-
D-3	80	18	2	-
S1-1	5	90	5	~1
S1-2	10	80	10	~1
S1-3	5	70	25	~1
S2-1	~1	5	90	5
S2-2	~1	10	80	10
S2-3	~1	10	70	20
B-1	-	-	1	99
B-2	-	-	5	95
B-3	-	1	9	90

## Appendix B – Calibration results

Results of the GC calibration experiments. Both the individual results of each parallel and the average, with the computed standard deviation below, are shown in table B-1.

**Table B-1: The results of the gas chromatograph calibration.**

	Individual samples				Average and standard deviations			
	meth	eth	prop	but	meth	eth	prop	but
D - Standard 1	40,923	28,729	-	-	19,357	13,459	-	-
	14,149	9,935	-	-	14,698	10,412	-	-
	7,859	5,279	-	-				
	14,495	9,892	-	-				
D - Standard 2	6,505	4,211	3,143	-	7,100	4,621	3,416	-
	9,035	5,787	4,493	-	1,291	0,782	0,725	-
	6,372	4,146	3,110	-				
	6,488	4,340	2,919	-				
D - Standard 3	6,628	4,390	3,164	-	4,402	2,907	2,209	-
	3,918	2,578	1,981	-	1,498	0,996	0,640	-
	3,431	2,275	1,864	-				
	3,630	2,386	1,828	-				
S1 - Standard 1	4,113	2,655	2,068	1,435	4,208	2,702	2,368	1,452
	3,881	2,525	1,832	1,415	0,263	0,144	0,714	0,039
	4,391	2,858	2,152	1,506				
	4,449	2,771	3,420	1,452				
S1 - Standard 2	4,763	2,980	2,317	1,660	4,584	2,825	2,168	1,587
	4,369	2,667	2,056	1,534	0,293	0,176	0,148	0,108
	4,900	2,974	2,274	1,693				
	4,303	2,679	2,027	1,462				
S1 - Standard 3	4,565	2,453	1,871	1,387	5,027	2,847	2,174	1,538
	6,945	4,106	3,123	2,105	1,292	0,841	0,634	0,380
	4,137	2,347	1,799	1,305				
	4,462	2,483	1,901	1,356				
S2 - Standard 1	5,955	3,529	2,573	1,942	12,830	5,079	3,563	2,779
	31,715	8,392	5,861	4,597	10,918	2,170	1,475	1,173
	6,093	2,915	2,119	1,683				
	12,805	5,868	4,045	3,217				
	7,584	4,693	3,215	2,456				
S2 - Standard 2	15,943	4,225	3,069	2,612	8,574	3,402	2,511	2,120
	6,596	3,276	2,459	2,083	5,104	0,885	0,618	0,525
	7,522	3,893	2,849	2,383				
	4,236	2,212	1,665	1,402				
S2 - Standard 3	4,987	2,419	1,815	1,587	6,601	2,622	1,858	1,597
	8,687	2,389	1,764	1,478	1,735	0,317	0,083	0,087
	7,357	3,075	1,923	1,657				
	5,375	2,605	1,932	1,667				
B - Standard 1	-	-	4,095	4,038	-	-	3,727	3,514
	-	-	2,851	3,007			0,762	0,516
	-	-	4,235	3,496				
B - Standard 2	-	-	2,703	2,466	-	-	3,293	2,909
	-	-	3,332	2,915			0,634	0,463
	-	-	4,163	3,547				
	-	-	2,975	2,710				
B - Standard 3	-	7,139	2,412	2,271	-	5,293	2,338	2,238
	-	3,925	1,993	1,837		2,178	0,622	0,592
	-	2,951	1,765	1,781				
	-	7,156	3,180	3,063				

## **Appendix C – Software descriptions**

In the simulations and calculations carried out in this thesis, a few computer programs were used. Some information on each is given here.

- Aspen Plus from Aspen tech. Version 2004.1.
- Lab VIEW from National Instruments. Version 8.2.1.
- Matlab from MathWorks. Version 7.1.